RSC Advances

ROYAL SOCIETY OF CHEMISTRY

www.rsc.org/advances

Journal Name

ARTICLE

Nano scale investigation of particulate contribution to diamond like carbon film by pulsed laser deposition

Madhusmita Panda,[a] G. Mangamma,[a] R. Krishnan,[a*] Kishore K. Madapu,[a] D. Nanda Gopala Krishna,[b] S. Dash[a] and A. K. Tyagi[a]

Diamond like Carbon (DLC) films were synthesized by Pulsed Laser Deposition technique at room temperature, with the laser pulse energy varying from 100 to 400 mJ. The films synthesized at different pulse energies are labeled as DLC-100, DLC-200, DLC-300 and DLC-400. Due to laser ablation, the DLC films contained a continuous phase and particulates embedded in it. These films were characterized using X-ray Photoelectron Emission Spectroscopy (XPS), Raman spectroscopy based intensity mapping and Atomic Force Acoustic Microscopy (AFAM). Carbon co-ordination inhomogeneity in DLC films was monitored by intensity mapping of the Raman peaks. The average sp^2 cluster size in the particulates were calculated from the intensity ratio of D and G peaks of the Raman spectra (I_D/I_G ratio) obtained from the particulate region and found to vary from 0.85 to 1.41 nm with various laser pulse energies. Nanometric surface spatial elasticity distribution was mapped using AFAM, which revealed presence of nanoscale surface irregularities in all the DLC films. The number density of particulates in the present DLC films is maximum in DLC-400 and minimum in DLC -100. Relative stiffness value of all the DLC films with its particulate regions were determined and compared with respect to the relative stiffness of Si. Raman spectroscopic intensity mapping and AFAM studies revealed carbon co-ordination and local elasticity distribution across the film and particulate of DLC films are observed to depend upon sp^2 bonded carbons possessing different aromatic orders and sp^3 content . The sp^3 bonding content present in DLC films synthesized at different laser pulse energies was obtained from X-ray photoelectron spectra. DLC-300 was found to be the stiffest film (~ 4.5 times of Si) with highest sp^3 content (53%).

Introduction

DLC is one of the exciting and highly sought after materials in industrial applications due to its high hardness, high elastic modulus, high electrical resistivity, good field emission, high thermal conductivity, high optical transparency and high chemical inertness.[1-4] DLC films are commonly used for cutting tools,anticorrosion coatings, tribological and electrochemical applications, in addition to various other applications such as protective layers in magnetic storage devices and micro-electromechanical systems (MEMS).[5-10] Properties of DLC are influenced by several features like; (a) sp^3 content, (b) H-content, (c) sp^2 cluster phase, (d) sp^2 cluster size, (e) number density of sp^2 cluster, (f) sp^2 cluster phase orientation and (g) any cross-sectional structure, as a consequence of interaction among sp^2 and sp^3 bonding of carbon.[11, 12] The above mentioned factors including chemical bonding of carbon atoms and mechanical properties like elasticity and hardness of the DLC

films depend upon the deposition method and the parameters used therein. [1, 2, 13, 14, 15, 16, 17] This is because energy of carbon species during deposition plays a vital role in establishing sp^3/sp^2 phase formation in the DLC films.[1, 2, 13] Pulsed laser deposition (PLD) has emerged as a successful deposition techniques to synthesize non-hydrogenated DLC (C-C sp^2 and sp^3 bonding) at room temperature. During the deposition, particulate (~ macro size) formation occurs on the surface of thin film due to heating of subsurface area by incidence of high power density (~ 10^9 W/cm^2) on the target surface. Presence of particulate influences the growth, morphology and surface mechanical properties of thin films. Particulate generation is more in Nd: YAG laser based ablation than excimer lasers due to its higher wavelength, which in turn make it more penetrating into the target surface.[1] The presence of particulates changes the film morphology and consequently the roughness also increases. In PLD, the kinetics and energetic of the plasma species produced by the laser impact play an important role in the formation of DLC film.[1, 2, 18, 19, 20] Quality of a DLC film deposited by PLD depends largely on energies and charge states of the ablated carbon particles in the plasma plume.[1, 2] Research groups like Tabbal et al., Yap et al. and Ruiz

a Materials Science Group, Indira Gandhi Centre for Atomic Research, Kalpakkam, 603102,India

b Corrosion Science and Technology Group, Indira Gandhi Centre for Atomic Research, Kalpakkam, 603102, India

et al. have carried out studies on DLC growth by PLD with parametric effects on its structural, optical, electrical and mechanical properties. These studies aimed to obtain high quality DLC films for appropriate applications.[2, 14, 18] Recently Ruiz *et al.* have studied elastic heterogeneities in nanostructured DLC films grown with various kinetic energies of ions ablated with an Nd: YAG laser of 1064 nm wavelength.[18] They have also studied sp^3 content variation along the thickness of the DLC films by angle resolved X-ray photoelectron spectroscopy and observed that sp^3content is less on the surface as comparedto the subsurface region. They found that DLC films synthesized with lowest kinetic energy (100 eV) of carbon ions with highest thickness (1050 nm) possess highest sp^3 content (40.8%) and all the films have an elastic heterogeneity extending only to 20 nm diameter size domains. The thicknesses of DLC specimens for higher kinetic energies (200 and 150 eV) were 350 nm and 650 nm, respectively. All these factors make it difficult to identify the dominant parameter (kinetic energy of carbon ions or thickness) that contributes to sp^3 content and consequently to elasticity of the surface. Hence, in this paper we have carried out a systematic study of DLC film formation with various laser pulse energies to obtain maximum sp^3 content, which will be suitable for hard coating related application. In addition, Young's modulus (measure of stiffness/ mechanical property) of DLC films has been reported to vary from 100-800 GPa and is a function of sp^3 tetrahedral bonds in the amorphous carbon network.[21-23] Nano-indentation is a widely used technique to determine the mechanical property of DLC films. However, in nano-indentation technique the maximum penetration depth should be less than or equal to 10% of the thickness to avoid any substrate effect, which can act as a limitation in case of thin films of few nanometers. Application ofDLC films demandssynthesis of films with various thicknesses starting from few nanometers to several micrometers. This requirement makes the hardness and elasticity measurements quite challenging. In this aspect, hybrid acoustic/AFM technique known as Atomic Force Acoustic Microscopy (AFAM) is a promising surface specific tool to map elasto-mechanical spread across a surface. This is a scanning probe microscopy basednondestructive technique designed to map elasticity distribution on a specimen surface.[24-26] Since, thin films grown by PLD using 1064 nm wavelength laser pulse possess particulates, it hinders local elastic mapping by AFAM at a constant contact resonance frequency. Hence, to overcome this, point spectroscopy method was adopted in AFAM to garner information about relative stiffness of particulate interior and exterior regions with respect to Si (111).

It is found from literatures, that many authors have adopted the method of incorporating (elements such as N, F, Si or metal, nanoparticles and nanocrystallites) at nanometric scale to improve the physical, mechanical and tribological properties of DLC for improved diverse applications.[27-31] In PLD systems like ours, which doesn't have sophisticated means for filtering particulates, we should investigate the role of particulates present in it, before incorporating such

nanoparticles. Hence in this report, evolution of carbon co-ordination in particulate region and its contribution to surface elastic inhomogeneity of DLC films at nanoscale, which were synthesized at various laser pulse energies, are probed. Study of surface elasticity variation along the particulates and flat regions are also mapped by AFAM mode under optimized SPM operating parameters. In this study, we have maintained most of the deposition parameters like target (target-substrate distance), laser type, wavelength, pulse duration, repetition rate and base pressure constant so as to bring out the co-relation of laser pulse energy with kinetic energy of carbon ions as reported earlier by Ruiz *et al.*.[18] This approach enables one to undertake qualitative study of evolution of carbon co-ordination distribution, morphology and surface elasticity inhomogeneity of nanostructured DLC films with particulates by two most sensitive and highly spatially resolving techniques like Raman mapping and AFAM imaging. These data were supplemented by quantitative analysis of sp^3 content by X-ray photoelectron spectroscopy (XPS). A few Raman imaging studies on DLC tribo films, reported in the literature, have already established it as a useful characterization tool to find out the phase change process (graphitization) occurring during tribological sliding.[32] We have also carried out Raman mapping of G peak, D-peak and corresponding I_D/I_G, respectively, by using a step size of 500 nm to obtain the local co-ordination of carbon atoms.

Experimental Section

DLC Specimen Synthesis by PLD

DLC films were synthesized on silicon (111) substrates having dimensions of 10×10 mm^2 by pulsed laser ablation from high pure graphite target with 10,000 laser shots. The Si substrates were cleaned with lukewarm soap solution, deionised water, acetone and ethyl alcohol for duration of 10 minutes per solvent successively in an ultrasonicator bath to remove surface impurities. The cleaned Si substrates were then loaded into laser ablation UHV chamber. An Nd: YAG laser (M/s Quanta Systems, Italy) operating at 1064 nm wavelength with maximum pulse energy of 900 mJ, pulse width of 5 ns and a repetition rate of 10 Hz was used. The area of laser spot was 0.7 mm^2. The deposition process was initiated after reaching a base pressure of 4.5×10^{-6} mbar and the deposition was carried out at 6×10^{-6} mbar at room temperature. The substrate to target distance was kept at 40mm. The laser pulse energy was kept at 100, 200, 300 and 400 mJ for the synthesis of films labeled as DLC-100, DLC-200, DLC-300 and DLC-400 specimens, respectively. The deposition of DLC films were carried out by exposing the 2" diameter pyrolytic graphite target (with purity close to 99.99 %) to the impacting laser pulses. Target was rotated continuously to expose fresh surface and to prevent pinhole formation.

Characterization Techniques

The thickness of the DLC films was measured by a profilometer (Dektak 6M stylus profiler, M/s Veeco, USA). A 12 μm diameter

of spherical diamond tip was line scanned on the DLC film surface with a speed of 15 μm /s to obtain the thickness. The normal load on the tip and scanning length for each measurement were 10 mg and 2000 μm, respectively.

XPS experiments were carried out using a SPECS manufactured (Germany) spectrometer employing monochromatic Al K_α (1486.74 eV) as the primary excitation source at room temperature. The anode was operated at a voltage of 13 kV and the source power level was set to 300W. The spectra were collected using the PHOIBOS 150 MCD-9 analyzer with a resolution of 0.67 eV for 656 kcps at pass energy of 10 eV and the data were processed by Casa XPS software. The analysis of each of the elemental carbon (1s) peak was deconvoluted after the subtraction of Shirley type background.

Raman spectroscopy (inVia, Renishaw) studies were carried out in backscattering configuration with Ar^+ laser excitation of wavelength 514.5 nm. This instrument is equipped with 1800 lines/mm grating and a thermoelectrically cooled CCD detector. In the present study, Raman intensity imaging technique was adopted along with the normal spectral acquisition. A 100X objective with numerical aperture value of 0.9 was used for collecting the spectra. The fully automated motorized specimen stage (Renishaw M/S20), having a spatial resolution of 100 nm, was used for the Raman intensity mapping. The Raman spectral mapping was performed by integrating intensities, which is essentially the peak intensity distribution corresponding to a particular wave number collected over a pre-defined area.[33, 34] Mapping was carried out with a spatial scanning step size of 500 nm in a region of 4×3, 6×4, 4×2, and 6×4 μm^2 belonging to DLC-100, DLC-200, DLC-300 and DLC-400 specimens, respectively, to include at least one particulate.

Elasticity mapping was carried out using an advanced multimode high resolution Scanning Probe Microscope (SPM) (NTEGRA Prima, M/s NT-MDT, Russia). A stiff cantilever was used in contact mode for AFAM study of DLC films along with Si as the reference. Both large area (5 × 5 μm^2) and small area (2.5 × 2.5 μm^2) scans were carried out to observe the uniformity and local structure of each film. In addition, roughness measurement was carried out using same cantilever tip. The cantilever has a stiffness constant of 30 N/m and dimension as 125×30×5 μm^3. Resonance frequency of the cantilever is about 330 kHz. In AFAM, the specimen was placed on the specimen stage with an ultrasonic transducer beneath, it vibrated in the frequency range of 0-5 MHz. The cantilever scans the specimen surface in contact mode through the tip. In this technique, the mechanical boundary conditions are guided by two kinds of interactions. First, interaction is nonlinear contact mode function of distance, which is due to mutual interaction between the tip and the film surface devoid of vibration. It becomes attractive at larger distances, becomes repulsive when the tip is in contact with the surface and increases rapidly when the tip is pressed against the specimens. Second, the longitudinal acoustic wave emitted from the transducer impacts the specimen which causes out-of-plane vibrations on the specimen surface leading to change in the mechanical boundary

conditions. The surface vibrations are transmitted into the cantilever via the sensor tip. Photo diode and a lock-in-amplifier are used to measure and evaluate the cantilever vibrations. Coupled modes of vibration specific to surface elasto-mechanical response are measured and a spatial elasticity map is eventually generated.[25, 26, 35, 36] In our study, presence of particulates (~ micrometers) restricts spatial elasticity mapping with accuracy so we carried out the AFAM study by mapping with magnitude of the coupled oscillation. Point spectroscopy technique was used to determine the relative stiffness of flat surface and particulate with respect to Si (111). In addition to AFAM, AFM images were also obtained between the tip and the film surface without any vibration.

Results and Discussion

A. Thickness and Roughness analysis

Average thickness, rate of deposition and root mean square (rms) roughness with error obtained from surface profilometer and AFM study, respectively, are shown in Table 1. It is observed from Table 1 that thickness increases monotonically with laser pulse energy. Surface roughness (rms) of DLC films increase with laser pulse energy due to the reasons discussed here. Higher pulse energy extricates larger material flux resulting in higher growth rate and thickness; it also makes particulate emission more probable, thereby causing surface roughness to go up.

Table 1. Thickness and surface roughness (rms) from Surface profilometer and AFM study, respectively.(Errors within bracket)

Specimen Name	Average Thickness (nm)	Deposition Rate (nm/shots)	RMS surface roughness (R_q) (nm)
DLC - 100	105(±3)	0.01(±0.0003)	1.5(±< 0.5)
DLC - 200	120(±5)	0.012(±0.0005)	2.7(±< 0.5)
DLC - 300	144(±12)	0.014(±0.0012)	3.3(±< 0.5)
DLC - 400	169(±13)	0.017(±0.0013)	4.5(±< 0.5)

B. Compositional Analysis

XPS analysis was used to obtain the sp^3 content in the DLC films. Fig.1 shows high resolution XPS spectra of carbon 1s (C1s) core level photoemission spectra from DLC films synthesized at different laser pulse energies. The C1s XPS peaks were deconvoluted into three distinct Gaussian–Lorentzian
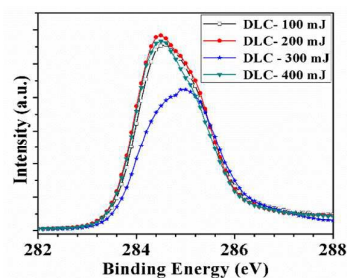

Fig. 1 XPS C 1s peak for DLC specimens at various laser pulse energies.

peaks after Shirley background correction (Fig.2a-d) and these were used for the estimation of sp^3, sp^2 and C-O bonding contents in the films.

It is observed from Fig. 1 that the line shape and peak position of the C1s peaks vary with the laser pulse energy. The line shape asymmetry stems from contribution of various chemical environments arising out of different hybridization states of carbon. The C1s peak position shifts towards higher binding energies and its shape tends to become more symmetric for DLC-300 specimen, indicating the transformation of sp^2 sites into sp^3 sites. The C1s peak position at lower binding energies and its asymmetric shape for DLC-100, DLC-200 and DLC-400 specimen indicate lower sp^3 content.

Fig. 2 shows the deconvoluted spectra of C1s peaks of DLC films deposited at different laser pulse energies. The first peak is located at 284.4 ± 0.1 eV and corresponds to sp^2 hybridized state of carbon atoms. The second occurs at a higher binding energy of 285.2 ± 0.1 eV and corresponds to sp^3 hybridized state of carbon atoms. The observed peak positions in the present study matches with the values reported in the literature for PLD grown DLC films.[2, 37] The third peak at the binding energy value of 286.2 ± 0.1 eV is due to C - O (or C =O) bond dominated chemical environment.[38] Fractions of sp^2 and sp^3 hybridized carbon atom are estimated from the ratio of the corresponding peak area to the total C1s peak area and tabulated in Table 2. Voevodin et al. reported that the sp^3 content of DLC films deposited by Nd-YAG laser is low.[1] The observed relatively low sp^3 content of the coatings in the present study is in agreement with Voevodin's observation. These observations point towards the growth of graphitic films and entrainment of particulates emitted by PLD process which employs 1064 nm Nd: YAG laser radiation at laser pulse power densities ≥ 10^9 Wcm^{-2}. Optimisation of the pulse energy to form DLC films leads to the conclusion that 300 mJ laser pulse energy is around the threshold energy to obtain a DLC film with maximum sp^3 content (53.47 %). This observation is comparable to the study of Ruiz et. al.[18]

From Table 2, it is clear that DLC-100 and DLC-200 specimens have sp^2 as the dominant phase fraction. This may be due to less kinetic energy of carbon ions in the plasma in comparison to threshold energy. However, there is a complete change of scenario in DLC-300 specimen, where sp^2 makes up only a fraction of 38.25 % and sp^3 becomes 53.47%. The sp^3 content in DLC-400 specimen is found to be similar to that of DLC-100 and DLC-200 specimens. Earlier studies on PLD grown DLC have indicated that the charge state and kinetic energy of carbon ions in the plasma plume determine the carbon co-ordination in thin film. [1, 19, 39] The sudden increase of sp^3 content in DLC-300 specimen is understandable with respect to sub-plantation theory. According to this theory, when kinetic energy of carbon ions in the plasma exceeds threshold energy, it penetrates into the thin film surface to achieve a dense film with substantially higher sp^3 content.[18]

As shown in table 2, the C and O bonding contribution is higher in DLC-300 as compared to DLC-100, 200 and 400 specimens. This indicates that the Carbon dangling bonds in

DLC-300 may more, which makes bonding with atmospheric oxygen during exposure. In case of DLC-100 and DLC-200 specimens, it can be predicted that lower energetic carbon ions in the plasma plume sticks to the surface without penetrating into the film and contribute more towards sp^2 bonding in the films. In case of DLC-400 specimen, though the laser fluence is highest which means that the plasma contains higher energetic and charge states of carbon species, it still has sp^3–content similar to that of DLC-100 and DLC- 200 specimens indicating that it does not follow the subplantation theory.[39] Hence, it can
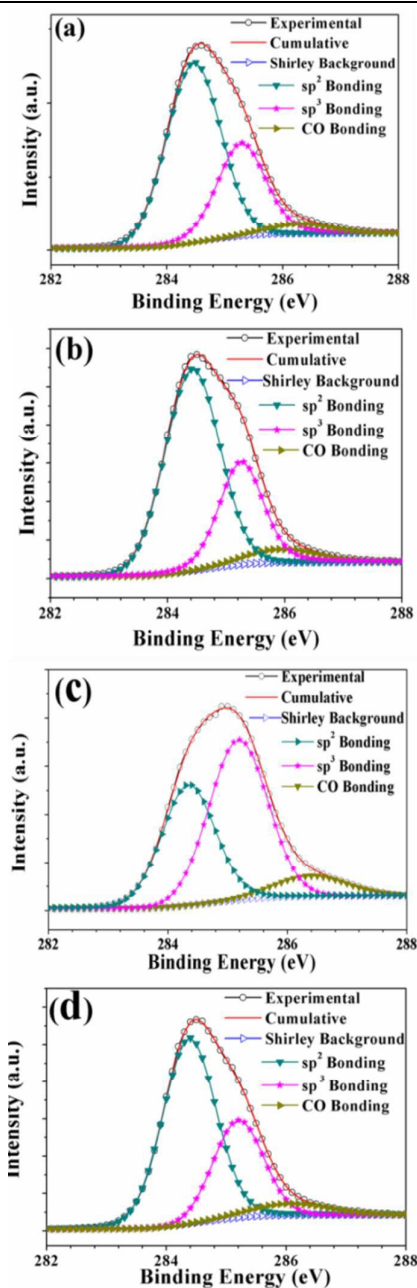

Fig. 2. XPS C 1s peak de-convolution for (a) DLC-100, (b) DLC-200, (c) DLC-300 and (d) DLC-400 films.

Table 2- XPS C 1s spectra de convolution results (Errors within bracket).

Specimen Name	sp^3 Band Position	sp^3 FWHM	sp^2 Band Position	sp^2 FWHM	C-O Band Position	C-O FWHM	sp^3 (%)	sp^2 (%)	C-O (or C=O) (%)
DLC-100	285.3(± 0.1)	1.0	284.5(± 0.1)	1.1	286.3(± 0.1)	1.3	32.3(±5%)	63.7(±5%)	4.0(±5%)
DLC-200	285.3(± 0.1)	0.9	284.4(± 0.1)	1.1	286.0(± 0.1)	1.4	29.1(±5%)	65.4(±5%)	5.5(±5%)
DLC-300	285.2(± 0.1)	1.1	284.3(± 0.1)	1.0	286.4(± 0.1)	1.4	53.4(±5%)	38.3(±5%)	8.3(±5%)
DLC-400	285.2(± 0.1)	1.0	284.4(± 0.1)	1.0	286.0(± 0.1)	1.5	30.5(±5%)	63.9(±5%)	5.6(±5%)

be speculated that the total kinetic energy of carbon ions in DLC-400 is not used to implant the ions in the subsurface of the thin film as in case of DLC-300. A fraction of the kinetic energy of carbon ions is used for other processes, like local heating due to dissipation of excess energy, following the thermal spike model causing sp^3 to sp^2 phase transformation.[2, 18] In addition, at higher laser pulse energies the particulate ejaculation is high, which hinders evolution of sp^3 phase as the graphitic matrix is retained as sp^2 phase on the film surface.[1, 19] Hence, it can be said that both the above mentioned phenomena have a combined effect on the film formation at 400 mJ.

In the following section, we have undertaken two mapping characterization techniques viz; visible Raman spectroscopic intensity mapping for local co-ordination and aromaticity of sp^2 bonded carbons in the particulates as well as on the surface and AFM morphology along with AFAM magnitude imaging for local elasticity distribution on surface to understand the XPS result by nanometric evolution process,.

C.   Structural Analysis

Raman spectroscopic imaging over the DLC film surface with a spatial scanning step size of 500 nm for determining local co-ordination of carbon in flat and particulate regions was carried out. Fig 3 (a, b, c, d) shows the optical images of the mapped area on the surface of all DLC films and the mapped area including particulate is shown as inset.

During the scanning, laser power was kept low (< 1 mW) to prevent laser induced damage of the specimen. The pre-selected area is different for different films (8 - 24 μm^2); hence number of acquired spectra varied from film to film.

All the mapped spectra corresponding to the DLC films were individually background subtracted and one of the Raman spectra obtained from the particulate region was deconvoluted into two Gaussian peaks corresponding to two distinct vibrational modes (G-band and D-band) of sp^2 – bonded carbon atoms. Usually the Raman spectra of disordered graphite exhibit two modes, the G peak (stretching mode) around 1550–1600 cm^{-1} and the D peak (breathing mode) around 1355 cm^{-1}, which are assigned to zone centre phonons of E_{2g} symmetry and K-point phonons of A_{1g} symmetry, respectively.[4, 11, 40-42]

Nanocrystalline and amorphous carbon phases are characterised by the position, intensity and widthof the G and
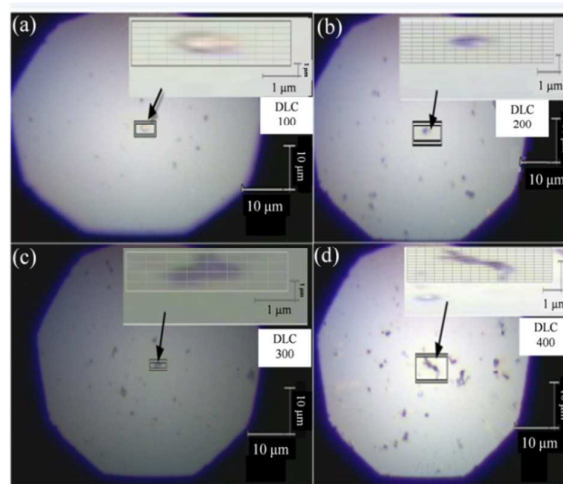

Fig. 3. Optical microscope images of (a) DLC-100, (b) DLC-200, (c) DLC-300 and (d) DLC-400 (inset-magnified image of mapped area)

D peaks in the Raman spectra. The G peak at 1581 cm^{-1} represents graphitic phase corresponding to E_{2g} symmetry and is associated with the in-plane bond-stretching motion of pair of sp^2 bonded carbon atoms. This mode does not require presence of six fold ring and is present in all sp^2 sites. The G band in the range of 1500–1630 cm^{-1} corresponds to sp^2 sites in aromatic and olefinic molecules.[4, 11, 43] The blue shift in G peak is due to smaller aromatic clusters having higher modes.[4, 11, 44] In addition, decrease in number of ordered aromatic rings on passing from nanocrystalline graphite to a-C also contributes to the blue shift of G-peak. It also reduces D peak intensity due to softening of the vibrational density of states.[4, 11, 45] Due to the higher sensitivity of visible Raman spectroscopy (50 – 230 times) towards sp^2 bonding than UV Raman spectroscopy, it is used as an indirect probing tool for sp^3 content.[4, 46, 47] In the following section, structural evolution of particulate region and their contribution to the DLC film with laser pulse energy variation are discussed.

Structural analysis of only Particulate region on DLC Films

In this section, structural evolution of particulate region and their contribution to carbon co-ordination on the film with laser pulse energy are discussed. Fig 4 (a, b, c, d) shows all the deconvoluted spectra obtained from the particulate regions. Peak position, FWHM of G and D peaks, I_D/I_G ratio, cluster size (effective crystallite size in the direction of graphite plane) and I_D/I_G ratio obtained from Raman spectroscopic mapping are tabulated in Table 3. I_D/I_G ratio of Raman spectra obtained from the particulateregion was used in Tuinstra and Koenig (TK) equation for second stage (nanocrystalline graphite to a-C) of amorphization trajectory to calculate the cluster size (L) in the DLC films.[4, 11, 48] The TK relations for second stage of amorphization trajectory is given as follows:

$$\frac{I_D}{I_G} = C(\lambda)L^2 \qquad (1)$$

$C(\lambda)$ is a constant and depends on the laser wavelength used for excitation (514.5 nm) and is 0.55 nm^{-2}. It is clear from the Table 3, that DLC-300 has the smallest sp^2 cluster (0.74 nm) embedded in the particulate region. This indicates that the sp^2 bonding of carbon atom in the particulate region of DLC-300 is more of chain type. However, particulate region of DLC-100, DLC-200 and DLC-400 possess higher cluster sizes1.23, 1.28 and 1.34 nm, respectively. This indicates that the sp^2 bonding of carbon atom in the particulate regions of DLC-100, DLC-200 and DLC-400 is in aromatic rings. Small cluster volume possibly arises from the presence of compressive stress.

From deconvoluted spectra, it is found that the G-Peak for all the DLC films lies in the range 1553 -1580 cm^{-1}, which is lower than that of the G-peak of graphite (1581 cm^{-1}). It is observed from Fig 4 (a, b, d) that D-peak starts appearing at 1379, 1410 and 1416 cm^{-1} in DLC-100, DLC-200 and DLC-400 films, respectively, with skewness associated with the G-peak. According to the report of Mapeli*et al.*, the upward shift of D-peak and presence of intense D-peak as a prominent shoulder in DLC-200 and DLC-400 clusters specimen indicate occurrence of large number of aromatics entrained in the particulate regions.[44] The decrease of D-peak intensity in the shoulder region and wave number shift towards a lower value 1360 cm^{-1} in DLC-300 concludes that the particulate region of DLC-300

possess as either reduced number of ordered aromatic rings or more number of olefinic carbon chains consisting of sp^2 bonds, which is in concurrence with the report of Beeman *et al.*.[45]
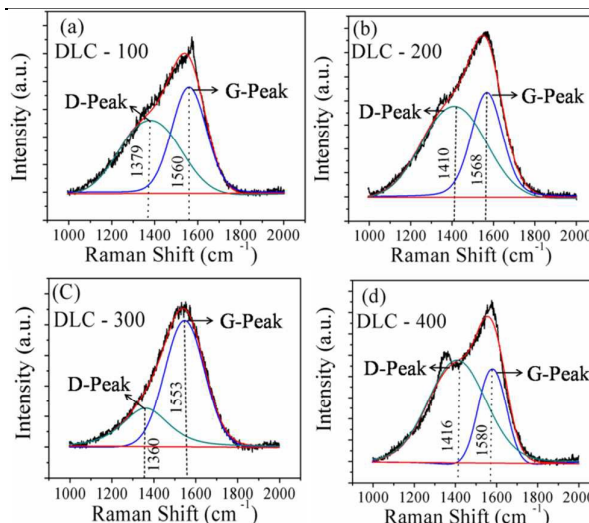

Fig. 4. Deconvoluted Raman spectra obtained from particulate regions of (a) DLC-100, (b) DLC-200, (c) DLC-300 and (d) DLC-400 films.

The relation between G-peak, D-peak and I_D/I_G ratio for the individual peaks obtained from particulate region is shown in Fig 5. According to the amorphous trajectory (Graphite→ Nanocrystalline graphite → a-C → TAC), G-peak position and I_D/I_G ratio from individual spectra (particulate region) of DLC-300 lie in the third stage of amorphization trajectory. This indicates that particulate region on DLC films are amorphous in nature with higher sp^3 content (> 20%).[11] Fig 6. shows the relationship between full width at half maximum (FWHM) of G-peak and I_D/I_G ratio obtained from the particulate region of DLC films at various laser pulse energies and the sp^3 content obtained from XPS study. FWHM of G-peak and sp^3 content of carbon shows similar trend whereas I_D/I_G ratio shows reverse trend, which also corroborates the fact that suddenly, sp^3 content increases with densification and amorphization at 300 mJ following subplantation theory for formation of DLC films and fails above it due to dissipation of the extra energy to the surrounding. The dissipation of extra energy in DLC films leads

Table 3- Raman spectra deconvolution results and cluster size obtained from I_D/I_G ratio of deconvoluted spectra and Raman spectroscopic mapping data of the DLC film.

| Specimen Name	G-peak position (cm^{-1})	G-peak FWHM (cm^{-1})	D-peak position (cm^{-1})	D-peak FWHM (cm^{-1})	I_D/I_G (Peak Intensity Ratio)	Cluster Size (nm)	I_D/I_G Total	Mapping data I_D/I_G Flat	I_D/I_G Particulate
DLC - 100	1560	190	1379	325	0.7	1.13	0.54 - 0.64	0.54-0.58	0.54-0.64
DLC– 200	1568	180	1410	360	0.9	1.28	0.50 - 0.66	0.60-0.65	0.50 - 0.58
DLC– 300	1553	213	1360	287	0.4	0.85	0.38 - 0.45	0.38-0.44	0.42 - 0.46
DLC– 400	1580	135	1416	338	1.1	1.41	0.60 - 0.75	0.60 -0.72	0.65 - 0.75

ARTICLE
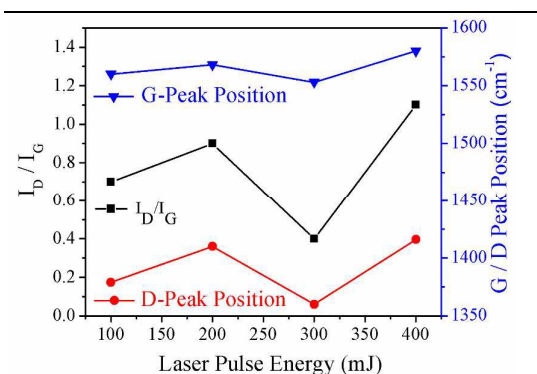
Fig. 5. Relation among G-Peak, D- Peak position and I_D/I_G ratio obtained from particulateregionsof DLC films at various laser pulse energies.

graphitization (conversion of sp^3 to sp^2 bonding).[18] The slight fall of sp^3 content for DLC-200 is the contribution from bigger size particulates than DLC-100. To study the contribution of particulate regions to DLC films, Raman spectroscopic intensity mapping was carried out and this is discussed in succeeding section.
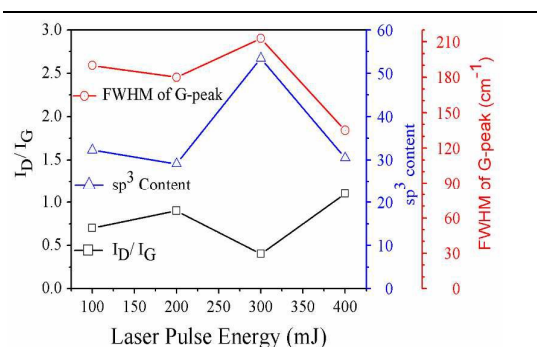

Fig. 6. Relation among FWHM of G-Peak, I_D/I_G (particulate region) and sp^3 content (XPS) of DLC films at various laser pulse energies.

Structural analysis of DLC Film (Including particulate region)

The Raman intensity mapping of G and D peak (obtained from deconvolution), and corresponding I_D/I_G ratio mapping for DLC-100, DLC-200, DLC-300 and DLC-400 specimens are shown in Fig 7 (a, b, c, d). It is observed from G, D and I_D/I_G ratio mapping that there is an intensity contrast from flat to particulate region in all DLC films. Here, it is focused on I_D/I_G ratio map of all DLC films, which provide the information about the presence of aromatic rings/chain type structures of sp^2 bonding in clusters as discussed earlier. In addition, qualitative analysis of sp^3 content and density of DLC films across its particulate regions with various laser pulse energies is also deduced from I_D/I_G ratio mapping.

According to McKenzie *et al.,* a local compressive stress is induced during deposition process due to high energetic ion bombardment, along with the shallow implantation ('subplantation') of incoming atoms.[49] As a consequence,

transition from sp^2 rich phase to stabilised sp^3 rich phase takes place at a critical compressive stress value (~ 4-5 GPa). However, J. Robertson stated that, energy of ion is responsible for subplantation, producing densification of the film thus promoting sp^3 content. Densification is the causative factor for evolution of compressive stress.[50]

I_D/I_G ratio map of Fig 7(a) reveals that particulate region of DLC-100 specimen possesses I_D/I_G ratio in the range 0.54-0.64 (violet-red colour) with a gradually increasing manner from centre towards the flat region having a lower range 0.54-0.58 (blue-black colour). Most of the flat regions correspond to I_D/I_G ratio (0.54-0.60). The above mentioned result illustrates that particulate region possess smaller sp^2 bonded aromatic carbon clusters (1.13 nm) with similar sp^3 content of the flat surface and embedded in it. [11, 50] In other words, it can be stated that the particulate regions possess similar compressive stress to the flat surface, which promotes densification as well as enhancement in sp^3 content.[49, 50]

I_D/I_G ratio map of DLC-200 specimen shown in Fig. 7(b) reveals particulate region exhibit similar contrast as the particulate region of DLC-100. In fact, the flat region has a variation in the higher range 0.50-0.65. Since, the particulate region of DLC-200 specimen have lower I_D/I_G value (0.50-0.58) with respect to the flat region, there is indication that smaller sp^2 bonded aromatic carbon cluster (1.28 nm) has a pronounced occurrence in these particulate regions than the flat region. I_D/I_G ratio map of the flat surface reveals a non-uniform distribution pattern. This pattern indicates that the particulate region and flat surface are under non-uniform compressive stress but with different value.[11, 50] As a result densification and sp^3 content varies accordingly.

I_D/I_G ratio map of DLC-300 specimen is shown in Fig.7(c).This reveals particulate region possesses the range 0.42 - 0.46 of intensity map. There is a gradual decrease of I_D/I_G ratio starting from the centre of the particulate region towards the flat region which indicates presence of uniform compressive stress and densification.[11, 50] The flat region of DLC-300 specimen has an I_D/I_G ratio value in the low range (0.38-0.44). Though in DLC-300 the particulateregions have higher I_D/I_G ratio value with respect to the flat surface, but it is less as compared to DLC-100 and DLC-200 specimens. This indicates that the particulate region of DLC- 300 specimen has larger aromatic clusters (cluster size ~ 0.85 nm) than the corresponding flat surface, which is smaller than DLC-100 and DLC-200 specimens. The I_D/I_G ratio for both flat and particulate regions of DLC-300 reveals that sp^3 content is more in comparison to DLC-100 and DLC-200 specimens.

I_D/I_G ratio map of DLC-400 specimen is shown in Fig. 7 (d). It reveals that the particulate region possess the intensity contrasts (0.65-0.75) in such a manner that the maximum (red colour) I_D/I_G value lies at the centre of the particulate region and it decreases gradually towards the flat surface (0.60-0.72). The higher I_D/I_G value of particulate region indicates that it has bigger aromatic sp^2 clusters (1.41 nm) with lower sp^3 content and density.[11, 50] The flat surface shows a similar pattern like DLC-200 specimen having lowest I_D/I_G value (0.60-0.72). The
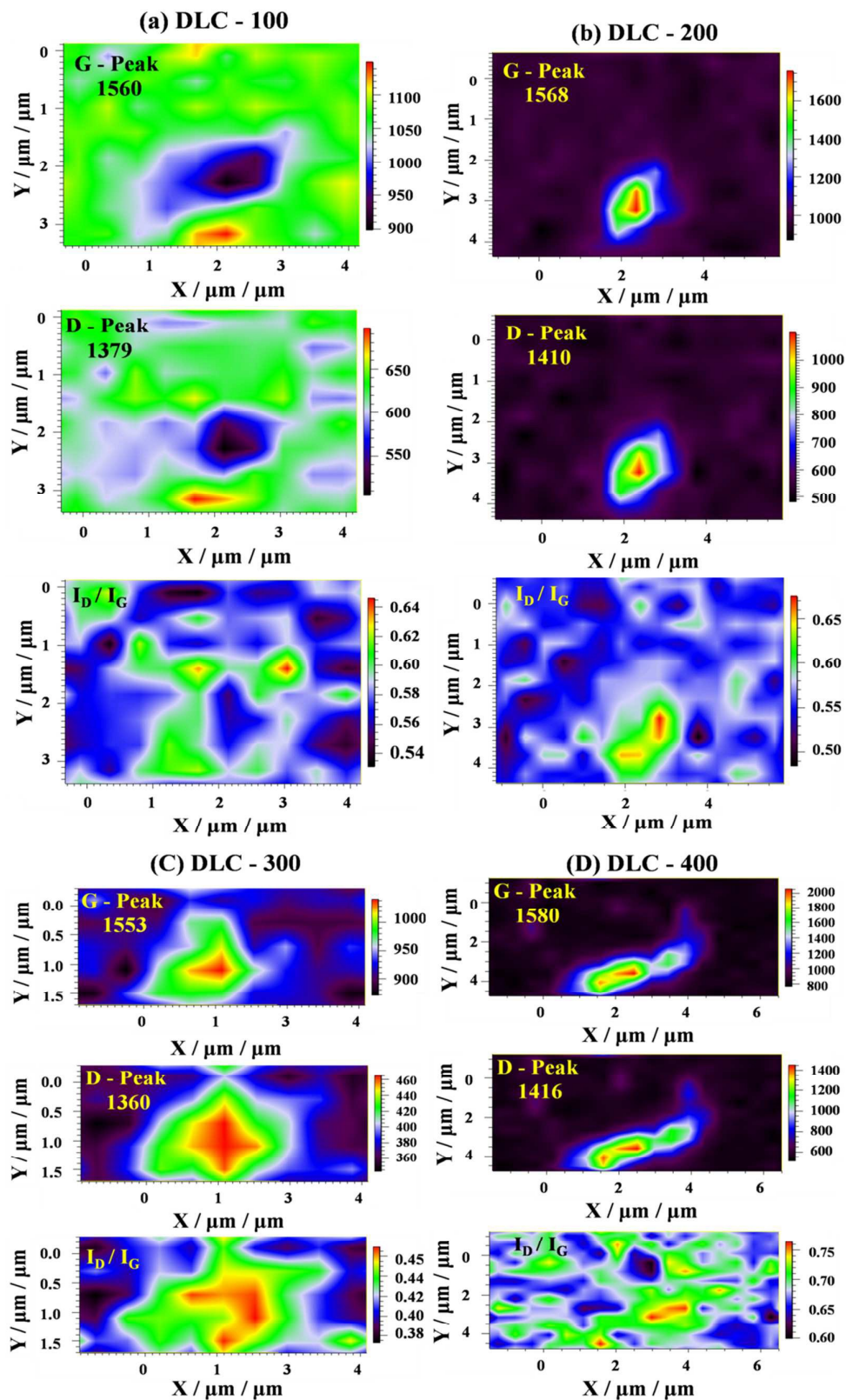
Fig. 7. Raman mapping image for G-Peak, D-Peak and I_D/I_G of (a) DLC-100, (b) DLC-200, (c) DLC-300 and (d) DLC-400, respectively.

ARTICLE

very high value of I_D/I_G on the flat surface indicates that DLC-400 has higher aromatic sp^2 clusters with less sp^3 content and density on the flat surface as compared DLC-100, DLC-200and DLC-300. In DLC-400 both flat surface and particulate region possess bigger sp^2 clusters than other DLC specimens, which decreases its sp^3 content and it's density.

D. Surface elasticity distribution Analysis

We have carried out local elasticity mapping of each specimen using AFM in contact mode as described in the experimental section. Prior to the experiment, AFAM imaging was carried out on "Si (111)" for reference. The large area (5× 5 μm^2) scan was done to see the uniformity of each DLC film and small area (2.5 × 2.5 μm^2) scan was carried out to observe the local structures present within the film. These results were compared with "Si" for morphology as well as AFAM imaging. Fig 8. depicts AFAM signal as magnitude (Mag), M.Cos (Magnitude x Cos) and phase along with AFM topography of Si substrate. More than one signal, M.Cos (Magnitude x Cos) is employed to improve the finer details present in the AFAM image. Si surface has an average roughness of ~1 nm and AFAM mapping clearly shows nano-micro-inhomogeneity with respect to local elasticity contrast.

AFM morphology and AFAM image (Mag) of all DLC films for both small area (2.5×2.5 μm^2) and large area (5×5 μm^2) scans are shown in Fig 9 (a, b, c and d) for DLC-100, DLC-200, DLC-300 and DLC-400 specimens, respectively. The magnitude variation is observed as dark and bright regions. The large change in the Mag image is mainly due to various types of particulate regions with different mass, size and shape distribution on the DLC film surface. This is attributed to discrepancy in elasticity among different particulate regions, their boundaries and also associated structures entrained within them. The purpose of this study is to determine surface elastic forces on flat surface and particulateregion of DLC films. The expression for stiffness

(K*) of the coupled oscillator system can be written as; [25, 26, 35, 36, 51]

$$K^* = 3\sqrt{(6RFE^{*2})} \qquad (2)$$

where, F, R and E* are the applied static force, radius of the sensor tip and the elastic constant of the tip and the specimen, respectively. E* is given as follows:-

$$\frac{1}{E^*} = \frac{1}{E_{tip}^*} + \frac{1}{E_{specimen}^*} \qquad (3)$$

Where, $\frac{E_{tip}}{(1-\nu_{tip}^2)}$, $E_{specimen}^* = \frac{E_{specimen}}{(1-\nu_{specimen}^2)}$

Here, "ν_{tip}" and "$\nu_{specimen}$" represent Poisson's ratios of tip and specimen, respectively.

The AFAM methodology uses contact resonance spectroscopy. When the cantilever tip comes in contact with the stiff region of the specimen surface, the frequency and amplitude of contact resonance curve gets enhanced while the FWHM decreases. The opposite happens when the tip is brought in contact with softer region. Hence, the choice of the operating frequency causes appropriate contrasting features to be exhibited. Operating frequency having a value higher than the resonance value causes stiffer region to appear bright and consequently softer region appears dark. However, if the operating frequency is lower than resonance frequency, a contrast inversion takes place causing stiffer region to appear dark and vice versa. This AFAM formalism is used to discriminate hard and soft regions.[36]

Mag image of Fig 9 (a) for DLC-100 specimen illustrates an elasticity contrast, where the softer regions are dark and the stiffer regions are bright. The contrasting features in DLC-100 specimen reveal two different observations. Contrast between smaller particulates and bigger particulate regions are clearly observed due to dissimilar relative stiffness values. This happens due to variation in densities and entrained subspecies.
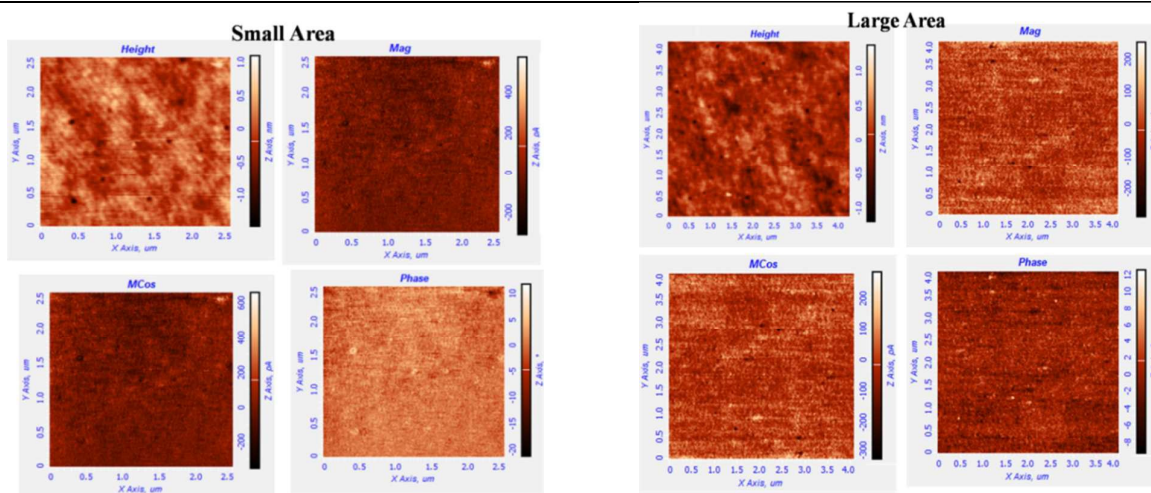

Fig. 8. AFM topography (Height) and AFAM (Mag, M.cos and Phase) images of Si (111) for small and large areas, respectively.

Hence, AFAM image specifically illustrates very small discrepancy in mechanical properties within small areas. The roughness of DLC-100 specimen obtained from AFM study is 1.5 nm.

Mag image of DLC-200 specimen is shown in Fig 9 (b). It shows that DLC-200 has softer regions as compared to that of DLC-100 which corresponds to dark region. This is owing to the increased laser pulse energy which enables ablation of higher sizeparticulates. It has been confirmed from XPS that DLC-200 has a higher sp^2 contribution than DLC-100. Since, DLC-200 has bigger particulates than DLC-100 as shown in Fig 9 (b). Therefore, it can be inferred that the occurrence of bigger particulates will lead to a higher sp^2 contribution. In addition, it is observed from AFM study that DLC-200 specimen has a

higher surface roughness (2.7 nm) as a result of bigger size of particulate.

Fig. 9 (c) and 9 (d) show number of particulates along with flat surface for DLC-300 and DLC-400 specimens, respectively. The roughness values of the DLC-300 and DLC-400 specimens obtained from the AFM study were found out to be 3.3 and 4.5 nm, respectively. This increase in roughness with laser pulse energy can be attributed to the presence of larger extent of soft zones as seen in AFAM images. In addition, it is also observedfrom Fig 9 (c) and Fig 9 (d) that the number of soft zones increases with increase in pulse energy. Therefore, DLC-400 has a higher number density of soft zones in comparison to DLC-300.

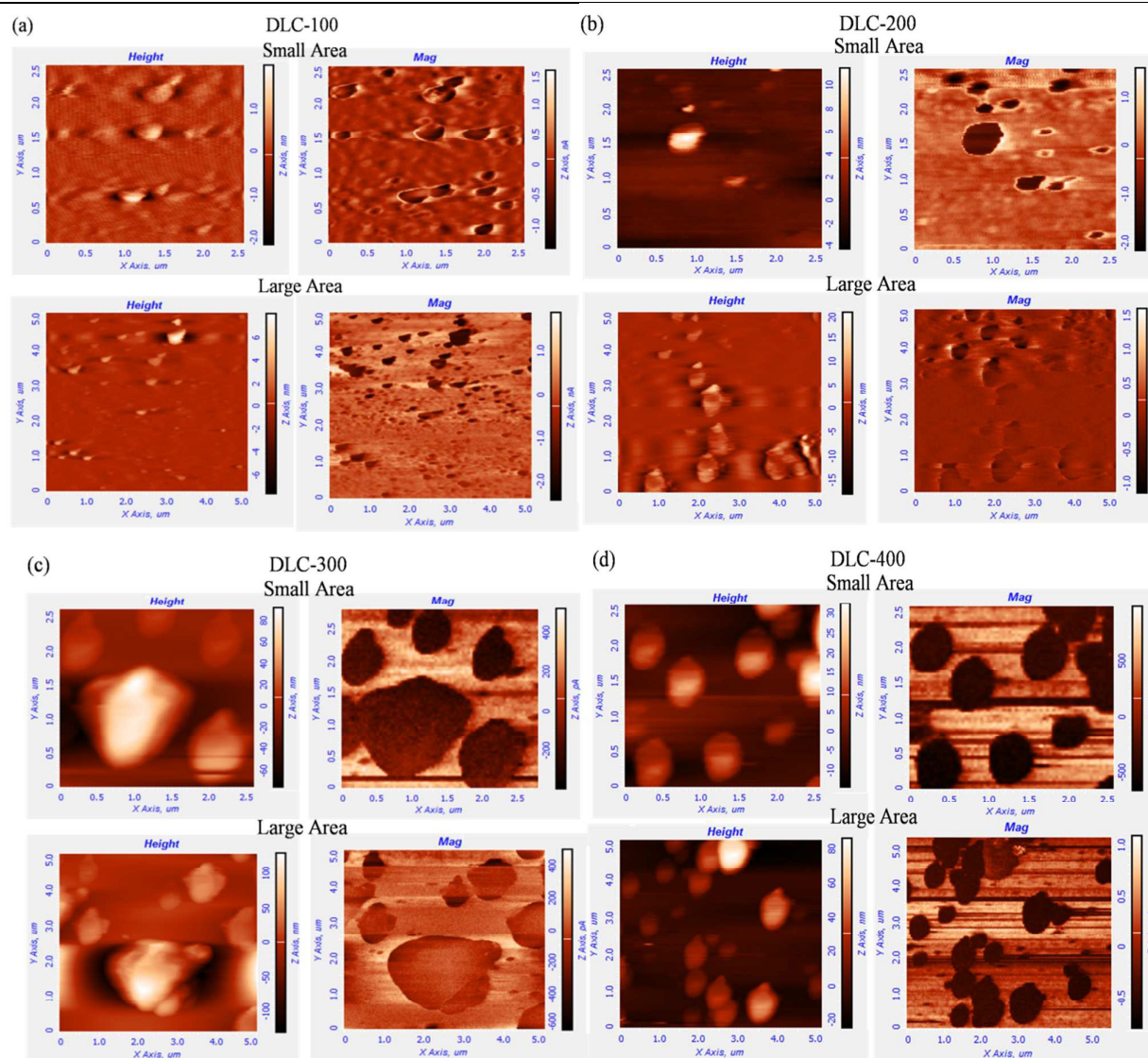Hence, it can be inferred that the dominance of soft phase

Fig. 9. AFM topography and AFAM (Mag) images for small and large area of (a) DLC-100, (b) DLC-200, (c) DLC-300 and (d) DLC-400, respectively.

brings down the relative stiffness value. The height contrasted AFM image has numerous contrasting features depicting spherically shaped particulate regions. The AFAM image is dominated with large number of elastically soft zones which eventually depresses the relative stiffness value.The contact resonance frequency of Si with known elastic constants and Poisson ratio was measured prior to commencing the measurements on the DLC specimens for contact resonance frequency and relative stiffness values. Mathematical expression for the contact resonance frequency of the coupled oscillator system is given by Eq. (4), [25, 26, 35, 36, 51]

$$f = f_0 \sqrt{\frac{K^* + K_c}{K_c}} \qquad (4)$$

Where f_0 is free oscillation frequency of the cantilever, K^* and K_c are stiffness of coupled oscillator system and the tip, respectively.

In this study, point spectroscopy method was adopted to avoid hindrances in set values during measurement of contact resonance frequency. This was necessitated due to the presence of particulates in DLC films. The relative stiffness of Si (111) and DLC-100, DLC-200, DLC-300 and DLC-400 specimens were calculated from the contact resonance frequency of cantilever. These values are listed in Table 4. The relative stiffness and contact resonance frequency of each film have been measured with respect to standard specimen Si (111). Table 4 depicts the behavior of relative stiffness variation on particulateregions and flat surfaces of DLC films with respect to laser pulse energy. The relative stiffness on flat surface of all DLC films except DLC-400 specimen has a higher value than that of Si (1.02). DLC-300 has the maximum value of relative stiffness (< 4.5818). In case of DLC-300 specimen, relative stiffness of flat region is 4.5 times higher than that of Si.

In case of DLC -100 specimens, particulate regions (2.3) show higher relative stiffness than that of flat region (1.8). This value is almost doubled with respect to Si. DLC-200 specimens show reverse trend as compared to DLC-100 specimen, which yielded higher relative stiffness on flat surface (2.2) as compared to particulate surface (1.7). DLC-400 has lower relative stiffness on flat surface and particulate region as compared to Si. This can be attributed to the presence of bigger particulates resulting in high density of defects as reported by Mangamma *et. al*..[36]

Contact resonance frequency of the cantilever on Si was measured each time before measuring the same on DLC films. This was done to achieve calibration of cantilever with respect to Si. Flat surfaces of all the DLC films (1116.1, 1108.74 and 1165.0 KHz) except DLC-400 specimen (957.13 KHz) have higher contact resonance frequency in comparison to Si substrates (1025.8 kHz). This indicates that flat surface of all DLC specimens (except DLC-400) have higher relative stiffness values than Si. In fact DLC-300 has relative stiffness 4.5 times of Si. DLC-400 specimen has a very low value of relative stiffness (0.5). Particulate regions of DLC-100 (1120 KHz) and DLC-200 (1093.05 KHz) have higher contact resonance frequencies with respect to Si, whereas DLC-300 (967.43 KHz) and DLC-400

(953.0 KHz) possess lower values. The observed relativestiffness in case of particulate regions of DLC-300 and DLC-400 films indicate that these are softer than those present in Si. Particulates of DLC-100 and DLC-200 films have higher relative stiffness with respect to Si but for DLC-300 and DLC-400, it is less than that of Si. All the relative stiffness results experimentally measured pertain to contribution from particulate number density and their size distribution across the surface. These aspects cause modification in contact stiffness of the cantilever.

Table 4- Contact Resonance and Relative Stiffness value of DLC films.

Specimen	Relative Stiffness	Resonance Frequency Shift (KHz)
Si	**1.02**	**1025.8**
DLC-100	**On Particulate** 2.3	**On Particulate** 1120
	On flat 1.8	**On flat** 1116.1
DLC-200	**On Particulate** 1.7	**On Particulate** 1093.05
	On flat 2.2	**On flat** 1108.74
DLC-300	**On Particulate** 1.0	**On Particulate** 967.43
	On flat 4.6	**On flat** 1165.0
DLC-400	**On Particulate** 0.4	**On Particulate** 953.0
	On flat 0.5	**On flat** 957.13

Generally particulates are softer than the flat region of the DLC films, because particulates are mostly made up of sp^2 clusters which are loosely packed in particulates than the flat surface. Again density of particulate varies with it's size, which affects it's stiffness. We observed that as the particulate size increases from DLC-1 to DLC -4, the measured relative stiffness decreases in the same manner indicating the decrease of density.

AFAM results of DLC films are similar to that of Raman mapping data. Relative stiffness of particulate regions and flat surface can be explained on the basis of aromaticity of sp^2 bonded carbons, cluster size, sp^3 content and density, as supported by Raman mapping and XPS studies. From Table 2, it is clear that thickness of a DLC film increases with increase in laser pulse energy, which in turn increases the density of DLC films and as a result relative stiffness should increase with laser pulse energy.[49] However, AFAM study of flat surface of DLC films reveals that the relative stiffness increases up to 300 mJ and above this, it shows a decline. XPS study shows a deviation from subplantation model for DLC-400 specimen having 30 % sp^3 content. DLC-300 specimen has highest sp^3 content of 53 %.

In addition, the evolution of I_D/I_G ratio (chain type/aromatic rings) and shift in G-peak position (cluster size) with laser pulse energy follow the same trend in line with the findings from AFAM and XPS.

Fig7. Reveals that, as seen from I_D/I_G ratio, all specimen, except DLC-400, follow the subplantation theory.[39] Hence, DLC-100 specimen all others possess higher I_D/I_G ratio for particulate region than flat surface. Similar result is also obtained from AFAM study. The particulate regions of DLC-100 specimen are stiffer than its flat surface, whereas the flat surfaces of other samples are stiffer than their particulate counterparts. This result is due to synergetic effect of density (size dependent), entrained substructures (clusters) and disorderedness (chain type or aromatic rings of sp^2 cluster) within the particulate regions, which is a consequence of intrinsic stress acquired during deposition. Crystalline diamond has only sp^3 bonding, which is very strong as a result diamond is hard. Whereas in polycrystalline diamond, grain boundaries instigate some sp^2 sites and other π-bonding states and introduces optical absorption subgroups. The stiffness depends on the fraction of C-C sp^3 sites, as only the sp^3 sites contribute significantly to the hard zones. In DLC, both sp^3 and sp^2 sites are present, which renders its electronic structure fundamentally different to ideal diamond.

The sp^2 sites have an inclination to form clusters to lower their free energy. DLC (or ta-C with lower C-C sp^3 content) is an atomically disordered alloy of sp^2 and sp^3 sites where the sp^2 sites are not strongly clustered. In this way, the density is linearly proportional to the sp^3 content as seen through experimentally and corroborated by earlier theoretical calculations. Hence higher C-C sp^3 fraction in DLC makes the material closer to diamond in terms of mechanical properties as revealed from AFAM, XPS and Raman spectroscopic studies. Both density and stiffness of films can be explained in terms of phase fraction of sp^2 and sp^3 types of carbon co-ordination.

The behaviour observed for DLC films with various laser pulse energies can be attributed to the synergistic effect of two factors, viz; (a) dissipation of extra energy (above threshold energy ~ 300 mJ) to the surrounding resulting transition of sp^3 to sp^2 bonding (graphitization process) and (b) number density and size of particulate regions entrained in each film.

Conclusion

DLC films of varying sp^3 content were synthesized at various laser pulse energies (100 – 400 mJ) with steps of 100 mJ. Quantitative and qualitative studies of sp^3 content were deduced from XPS and Raman spectroscopy, respectively. XPS study revealed that DLC-300 possesses highest sp^3 content (53%), whereas other DLC films possess a sp^3 content of ~ 30%. In our study, the evolution of sp^3 content follows the subplantation model up to DLC-300 and fails for energies beyond it. The average cluster size calculated from I_D/I_G ratio obtained from the particulate region varies with laser fluencies as 1.13, 1.28, 0.85 and 1.41 nm. The relative stiffness constants of all DLC-films (except DLC-400) are more with respect to Si, which indicates that DLC-400 is very soft. In case of DLC-300 the

relative stiffness is very high as compared to Si, which is about 4.5 times higher but the bigger particulate regions are very soft. It is observed that 300 mJ laser pulse energy is the threshold energy for obtaining highest sp^3 content and relative stiffness. It is also found that the bigger particulate regions are soft in comparison to small ones owing to poor density and higher number of defect states. In this study, it has been pertinently pointed out that AFAM is an effective technique to find out the nanoscale mechanical property.

Acknowledgement

References

1. A.Voevodin and M. Donley, Surf. Coat. Technol., 1996, 82,199.
2. M.Tabbal, P.Merel, M.Chaker, M.Khakani, E.Herbert, B.Lucas, and M. O. Hern, J.Appl. Phys., 1999, 85, 3860.
3. W. S. Choi, M. Park and B. Hong, Thin Solid Films, 2007, 515, 7560.
4. J.Robertson, Materials Science and Engineering R,2002, 37, 129.
5. T.C.S. Vandevelde, K. Vandieredonck, M.V. Stappen, W.D. Mong and P. Perremans, Surf. Coat. Technol., 1999, 113,80.
6. L.K.Meyer and R. Hauert, Thin Solid Films, 1999, 338,172.
7. B.Bhushan, Diam. Rel. Mater, 1999, 8, 1985.
8. Stephane Neuville, QScience Connect, 2014, 8.
9. B.Cord and J.Scherer, IEEE Trans Mag., 2000, 36, 67.
10. B.Bhushan, Handbook of Micro – Nanotribology, CRC, Boca Raton, FL, USA, 1999.
11. A.C. Ferrari and J. Robertson, Physical Review B, 2000, 61, 14095.
12. A.C. Ferrari and J. Robertson, Physical Review B, 2001, 64, 075414 1.
13. J. Robertson, Pure Appl. Chem, 1994, 66, 1789.
14. S. S. Yap, W.O. Siew, C.H. Nee and T.Y. Tou, Diamond & Related Materials, 2011, 20, 294.
15. D. Sarangi, O. S. Panwar, S. Kumar, and R. Bhattacharyya, J. Vac. Sci. Technol. A , 2000, 18, 5,2302.
16. O.S. Panwar, Mohd. Alim Khan, Mahesh Kumar, S.M. Shivaprasad, B.S. Satyanarayana, P.N. Dixit, R.Bhattacharyya, M.Y. Khan, Thin Solid Films, 2008, 516, 2331.
17. O. S. Panwar, M. A. Khan, B. S. Satyanarayana, R. Bhattacharyya, B. R. Mehta, S. Kumar and Ishpal, J. Vac. Sci. Technol. B, 2010, 28.
18. F.J.F. Ruiz, A.H. Gomez, E. Camps and F.J. E.Beltran Mater. Res. Express, 2015, 2, 025009, 1.
19. H.C. Ong and R. P. H. Chang, Physical Review B., 1997, 55, 13, 213.
20. A. A. Voevodin, M.S. Donley and J.S. Zabinski, Surf. Coat. Technol,1997, 92, 42.

Please do not adjust margins

RSC Advances

ARTICLE

21. B. Schultrich, H.J. Scheibe, D. Dresher and H.Ziegle, Surf. Coat. Technol., 1998, 98, 1097.

22. A.C. Ferrari, J. Robertson, M.G. Beghi, C.E. Bottani, R. Ferulano and R. Pastorelli, Appl. Phys. Lett., 1999, 75, 1893.

23. J.W. Chung, C.S. Lee, D.H. Ko, J.H. Han, K.Y. Eun and K. R. Lee., Diam. Rel. Mater., 2001,1,2069.

24. U. Rabe, S. Amelio, E. Kester, V. Scherer, S. Hirsekorn and W. Arnold, Ultrasonics, 2000, 38, 430.

25. D.C. Hurley, N.M. Jennett and J.A. Turner, J. Appl. Phys., 2003, 94, 2347.

26. F. Marinello, P. Schiavuta, S. Vezzù, A. Patelli , S. Carmignato, and E.Savio., Wear, 2011, 271, 534.

27. Q. Wei, A.K. Sharmaa, J. Sankara, J. Narayana, Composites B, 1999, 30, 675.

28. Alfred Grill, Diam. Rel. Mater., 1999, 8, 428.

29. Ishpal, O.S. Panwar, A.K. Srivastava, Sushil Kumar, R.K. Tripathi, Mahesh Kumar, Sandeep Singh, Surface & Coatings Technology 206, 2011, 155.

30. O.S. Panwar, Sushil Kumar, Ishpal, A.K. Srivastava, Abhilasha Chouksey, R.K. Tripathi, A. Basu, Materials Chemistry and Physics 132, 2012, 659.

31. R.K. Tripathi, O.S. Panwar, A.K. Srivastava, Ishpal Rawal, Sreekumar Chockalingam, Talanta 125, 2014, 276.

32. S. Kataria, S. Dhara, H.C. Barshilia, S. Dash, and A.K. Tyagi., Journal of Applied Physics, 2012, 112, 023525, 1.

33. K. K. Madapu, N. R. Ku, S. Dhara, C. P. Liu and A. K.Tyagi, J. Raman Spectrosc., 2013, 44, 791.

34. A. Patsha, K.K. Madapu and S. Dhara, MAPAN-Journal of Metrology Society of India., 2013, 28, 279.

35. U. Rabe, S. Amelio, M. Kopycinska, S. M. Hirsekorn, M. Kempf Goken and W. Arnold, Surf. Interf. Anal. 2002, 33, 65.

36. G. Mangamma, K.K. Mohan, M.S.R. Rao, S. Kalavathy, S. Dash and A. K. Tyagi, Journal of Nanoscience and Nanotechnology, 2007, 7, 1.

37. J.M. Lackner, C. Stotter, W. Waldhauser, R. Ebner, W.Lenz and W.Beut. Surface and coatings Technology, 2003, 174, 402.

38. T. Leung, W. Man, P. Lim, W. Chan, F. Gaspari and S. Zukotynski., Non-Cryst. Solids, 1999, 254, 156.

39. Y. Lifshitz, G.D. Lempert, E. Grossman, I. Avigal, C. U. Saguy, R. Kalish, J. Kulik, D. Marton and J. W. Rabalais., 1995, 4,318.

40. F. Tuinstra and J. L. Koening , Phys. 1970, 53, 1132.

41. R.J. Nemanich and S.A. Solin., Phys. Rev. B, 1979, 20, 392.

42. P. Lespade, R. AlJishi, and M.S. Dresselhaus, Carbon, 1982, 20, 427.

43. D. L. Vien, N.B. Colthurp, W. G.Fateley and J.G. Grasselli, The Handbook of Infrared and Raman Characteristic Frequencies of Organic Molecules, Academic, New York, 1991.

44. C. Mapelli, C. Castiglioni, G. Zerbi and K. Mullen, Phys. Rev. B 1999, 60, 12710.

45. D. Beeman, J. Silverman, R. Lynds, and M.R. Anderson, Phys. Rev.B, 984, 30, 870.

46. N. Wada, P. J. Gaczi, and A. Solin, J. Non-Cryst. Solids, 1980, 35-36, 543.

47. S.R. Salis, D. J.Gardiner, M. Bowden, J. Savage, and D. Rodway, Diamond Relat. Mater, 1996, 5, 589.

48. A.C. Ferrari and J. Robertson, Phil. Trans. R. Soc. Lond. A, 2004, 362, 2477.

49. P.C. Kelires, Diamond Relat. Mater, 2001, 10, 139.

50. J. Robertson, Diamond and Related Materials, 1993, 2, 984.

51. M. Muraoka and S. Komatsu, Nanoscale Res. Lett., 2011, 6, 33.

<u>Table of content / Graphical Abstract</u>
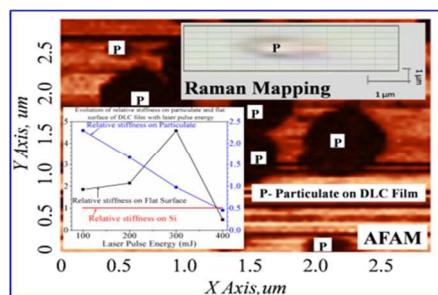
Raman mapping and AFAM are useful tools to evaluate the relative stiffness of DLC films embedded with micro graphitic particulates.